






## Research Article

# Numerical Study on the Thermal Enhancement of Phase Change Material with the Addition of Nanoparticles and Changing the Orientation of the Enclosure

P. Narasimha Siva Teja <sup>1</sup>, S. K. Gugulothu <sup>1</sup>, P. Dinesh Sankar Reddy <sup>2</sup>, Abdul Ashraf,<sup>1</sup>  
B. Deepnaraj <sup>3</sup> and P. Thillai Arasu <sup>4</sup>

<sup>1</sup>Department of Mechanical Engineering, National Institute of Technology, Andhra Pradesh, India

<sup>2</sup>Department of Chemical Engineering, National Institute of Technology, Andhra Pradesh, India

<sup>3</sup>College of Engineering, Prince Mohammad Bin Fahd University, Al Khobar, Saudi Arabia

<sup>4</sup>College of Natural and Computational Science, Wollega University, Ethiopia

Correspondence should be addressed to P. Thillai Arasu; [thililaiarasu@wollegauniversity.edu.et](mailto:thililaiarasu@wollegauniversity.edu.et)

Received 1 April 2022; Accepted 9 May 2022; Published 6 June 2022

Academic Editor: Zafar Said

Copyright © 2022 P. Narasimha Siva Teja et al. This is an open access article distributed under the Creative Commons Attribution License, which permits unrestricted use, distribution, and reproduction in any medium, provided the original work is properly cited.

The global demand of the heating and cooling applications gives a larger potential to study the thermal energy storage system. Phase change materials (PCM) that are used to charge, store, and discharge the heat energy are inferior in heat transfer characteristics. The properties of PCM can be improved by adding nanoparticles, changing the orientation of the enclosure or both. Two-dimensional transient numerical analysis on the effect of Grashoff number (5000, 13000, and 20000), nanoparticle type ( $\text{Al}_2\text{O}_3$ , CuO, and MWCNT), and volume concentration (0%, 1%, 3%, and 5%) added in RT 42 PCM and orientation of square enclosure (30, 45, and 60°) to enhance the heat transfer rate is carried out. The thermophysical properties of the nano-PCM are evaluated and presented. From the results, it is affirmed that the melt fraction of the PCM rises with the increase in Gr and volume concentration of the nanoparticles up to an optimum level. The MWCNT-based nano-PCM attained a larger portion of melt fraction followed by  $\text{Al}_2\text{O}_3$ , CuO, and pure PCM. It is noted that an orientation of 60° and 45° will convert more quantities of pure PCM and nano-PCM into liquid fraction, respectively. The (3% MWCNT/RT-42 PCM) filled in 45° oriented container attained the highest melt fraction by 3.4%, 2.04%, and 2.94% than (3%  $\text{Al}_2\text{O}_3$ /RT-42 PCM), (1%CuO/RT-42 PCM), and pure PCM. The variation in the maximum melt fraction of the nanomaterial is because of the change in thermophysical characteristics of the nano-PCM.

## 1. Introduction

Renewable energy resources are emerging in the present world to reduce global pollution and replace a portion of conventional fuels. Thermal energy having various industrial and domestic applications can be substituted with solar heat energy which is one of the prominent renewable energy sources. This energy is intermittent and depends on weather conditions. Therefore, storage of low-grade energy is inevitable to provide a sustainable solution to energy demand. Thermal energy storage can be done by using latent heat materials by changing their phase. Also, PCMs can be used

in thermal management of different heat transfer applications like electronic cooling, waste heat recovery. Despite the larger heat capacities of phase change materials (PCM), it has a drawback of inferior heat transfer characteristics. Hence, improving the thermal characteristics of PCM is a challenging area in this field. Numerical assessment on thermal conductivity improvement of the PCM under uniform and sinusoidal types of heat flux by incorporating multi-walled carbon nanotubes was carried out by Gupta et al. [1]. An increase in melting rate was observed for higher values of amplitude and wavelength ratio of undulations applied on the vertical wall of the square duct. The charging

process of the thermocline storage tank (TCST) was studied both experimentally and numerically by Xu et al. [2] by developing a 1D model. They introduced the correction coefficient ( $\varepsilon$ ) expresses the enhancement in thermal diffusion. The use of the 1D model predicted the distribution of temperature more accurately and developed a correlation equation between the thickness of thermocline,  $Fr$ , and  $Re$ . They reported analytical expression between thermocline thickness and time is also obtained with approximately 14% of error. Experimental and computational investigations on the theory of constituent mixtures in the PCM composites were performed by Jiao et al. [3]. In this, the effect of nonequilibrium mixtures and the relation between velocity and change in density during melting were discussed. The temperature contours and streamlines are presented. The numerical and experimental results are compared for different positions and achieved a good agreement. Melting rate analysis of an encapsulated PCM incorporated with metal foam was done numerically by Baruah et al. [4]. The parameters varied in this study are porosity, pore size distribution, capsule size, and thickness of shell. They observed that the melting rate is improved for minimum capsule size and porosity with higher shell thickness. Computational study on the effect of encapsulated geometry filled with PCM for different angular orientations has been carried out by Zhang et al. [5]. They observed that the pyramidal and tetrahedral-shaped capsules with a horizontal base have the highest melting rate due to larger surface area. Comparing angular inclination, the melting rate is more when the center of gravity of capsules was nearer to the bottom of geometry. Huang et al. [6] inspected the rate of melting of double-PCM heat sinks by mixing paraffin with an alloy having lower melting point (LMPA). The performance characteristics are evaluated for different volume fractions of LMPA, the fin shape, and heating power. They reported that, throughout the second melting stage, the double-PCM heat sink and LMPA heat sink were similar in performance. However, during the third melting stage, the temperature control with paraffin gets deteriorated. The fin shape and volume fraction of the LMPA have been optimized by extending the second stage of melting and eliminating the third melting stage. Experimental assessment of the heat transmission enhancement of PCM-based heat energy storage system and its allied applications by incorporating metal fins and foams is performed by Guo et al. [7]. They affirmed that the combination of fin and foam structure reduces the melting time by 83% than bare, ideal fin, or metal foam structures. The uniformity of the temperature field is maintained with the help of foam structure only but not with the fin structure. Nie et al. [8] inspected the impact of geometry with seven different vertical-shell tubes on heat transmission characteristics in a latent thermal energy storage network. They reported that frustum-shaped geometry enhanced both conduction and convection, while the conical shell improved only convection compared to cylindrical geometry. Geometry modification has little effect on heat transfer in composite metal foam/PCM. The impact of thickness and position of the PCM film, different climatic conditions, PCM melting point temperature on the heat transfer analysis in the thermally

efficient building are performed by Li et al. [9]. Results suggested proper melting point PCM reduces temperature fluctuations and energy expenditure of air conditioning units, and higher input temperature requires higher melting point PCM. Also, the PCM with melting point near to the occupant's comfort zone increases the thermal comfort especially at moderate climate conditions. Huang et al. [10] evaluated the heat transmission improvement in the composite type PCM by incorporating porosity of metal foams having high conductivity. They noted that the rate of PCM melting is increased with foam porosity. Computational and experimental investigations on the impact of heat sink orientation attached to the PV cell passive cooling system are conducted by Abdulmunem et al. [11]. The heat sink is filled with PCM and studied with different inclinations of  $0^\circ$ ,  $30^\circ$ ,  $60^\circ$ , and  $90^\circ$ . They observed that the PCM melting speed has been enhanced alongside the advancement of orientation angle from  $0$  to  $90^\circ$ . The heat transmission analysis of the rectangular latent thermal energy storage network with different partitions (1, 2, 4, 8, 16, and 32) was performed experimentally (1 and 2 partitions) and numerically (for other partitions) by Mahdi et al. [12]. Partitioning of LHSU led to an increase in PCM melting speed, and a partition of 8 was found as the optimum. The amount of increase in melting rate is 31%, 53%, 65%, and 68% for 2, 4, 8, and 16 partitions compared to a single partition. Simulation study of integrated PCM partition and heat transmission fluid is conducted by Sodhi and Muthukumar [13]. The phase change materials selected in this analysis are in the range of  $360^\circ\text{C}$  to  $305^\circ\text{C}$ . The impact of Fin distribution, Stefan number on heat energy transmission was carried out. They noted that, for  $Ste_{ref} \geq 1$ , the m-PCM system has the same or lesser charging or discharging rate than a single PCM system. However, there was an improvement up to 25% for  $Ste_{ref} = 0.5$  to 2. Employing different fin-distribution and ratio of PCMs block length reduced the time for charging and discharging as high as 30% compared to a single PCM system. Performance analysis of different PCMs with higher and lower melting temperatures for PVT applications for weather conditions of Iraq in summer is published by Chaihan et al. [14]. The materials selected are paraffin wax, Vaseline-petroleum jelly, and its combination. The outcomes exhibited that the hybrid PCM using Vaseline completely mixed with paraffin wax is formed with a lower melting point. Usage of petroleum jelly, paraffin, and hybrid paraffin (50%wax + 50%Vaseline) in the PVT structure caused a reduction in photovoltaic cell temperature, which led to huge improvements in efficiency of the system. Experimental investigation of a 2-phase closed thermosyphon (TPCT) form of heat pipes is done by Ozbas et al. [15]. The impact of the number of pipes at different positions (types 1, 2, and 3) and different angles of inclinations ( $26^\circ$ ,  $41^\circ$ , and  $56^\circ$ ) on the effectiveness of TPCT is studied. They found that the best results are obtained for  $26^\circ$  and also affirmed that the greater the tilt angle the greater thermic resistance with lesser heat transferability of TPCT. Numerical analysis of melting and heat energy transmission of PCM

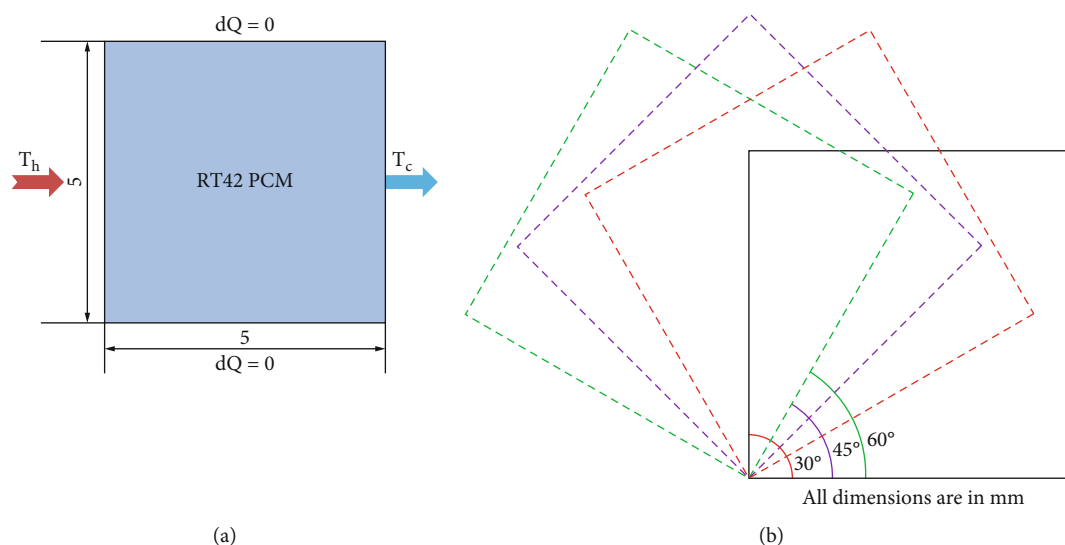


FIGURE 1: (a) Model geometry with horizontal and vertical sides. (b) Orientation of the enclosure.

in a rectangular block with bilateral flow has been done by Qin et al. [16]. The analysis was done by varying the values of Re number of heat transfer fluids ranging from  $10^4$  to  $7 \times 10^4$  and Ra number in range of  $3 \times 10^6$  to  $6 \times 10^6$ . They reported that the development of natural convection mode is owing to the effects of abnormal HTF heat transmission and cooling among the solid-liquid and the liquid PCM. Investigation on the effect of melting performance of paraffin RT82 PCM with distribution of copper-oxide-nanoparticles (CuO) at varying concentrations has been performed in multitube heat exchange units by Bashirpour-Bonab et al. [17]. The effect of nanoparticle mixture upon flow structure and heat transmission characteristic at different stages of melting of PCM was studied. They observed that with the increase of nanoparticles concentration between 3 and 7% leads to reduction in the time taken for melting by 8.7% to 22.18% though there is a minimal effect in the prime melting stages. It is also noted that the number of internal tubes has positive effects in melting rate and negative effects with distance between the tubes. Gollapudi et al. [18] numerically explored the impact of horizontal fin in a square container packed with  $Al_2O_3$  nanofluid and found that heat transmission characteristics were upgraded with the presence of fin. Additionally, higher conductivity ratio of fins resulted in better heat transmission performance. De Césaró Oliveski et al. [19] investigated the melting method of lauric acid inside a rectangular shaped container with extended surface. The parametric study was performed for 78 different configurations by only changing the fin aspect ratio. They concluded that the total melting time reduced with decrease in aspect ratio of the fin. With increasing value of volume concentration ( $\phi$ ), there was an increase in rate of melt fraction. Furthermore, it is observed that there is a drop in energy accumulation as the value of  $\phi$  rises. Abidi et al. [20] simulated the charging and discharging procedure of  $CaCl_2 \cdot 6H_2O$  PCM containing graphene

in 2D enclosed circular space. The enclosure contains two circles. The inner circle containing 12 blades of rectangular shape incorporated was kept at higher temperature for charging and lower temperature for discharging. The results show that increase in blade length caused a rise in enclosure temperature in charging mode and with a blade length of 1.5, and the Nu is enhanced by 252% in the first 100 s and decreased by a factor of 0.87 in 1000 s while charging whereas it is reduced by 94% and increased by 115% for discharging mode. Computational evaluation on thermal energy storage network employing fins with linear tree-like shapes with the integration of  $MoS_2$ - $TiO_2$  hybrid nanoparticles termed as hybrid nanoenhanced phase-changing material (HNEPCM) was done by Hosseinzadeh et al. [21]. It was found that the tree-shaped fins achieved superior heat transmission characteristics than rectangular fins and absence of fins. Evaluation of enhancement of melting characteristics of PCM by accommodating a new fin design is conducted by Kok [22]. Both types of fins are compared using base and nano-PCMs. They concluded that incorporating heat transfer fins improved the melting rate as well as reduced the cost and weight of thermal energy storage systems (TES). The designed fin reduced the melting time by 63% in the thermal energy storage tank. Design and analysis of a PCM-filled square cavity with thermal heat flux at distinct sites (0.2 L, 0.4 L, 0.6 L, and 0.8 L) were done by Dora et al. [23]. A heating element was positioned at the lowest surface with different locations varied in terms of length. The transient analysis was done for 10 hrs. They concluded that the heater at 0.2 L and 0.4 L assured the complete melting of the PCM than other locations. Experimental analysis was directed by Jevnikar and Siddiqui [24] to know the thermal behaviour of phase change material while melting. The temperature and velocity are measured using thermocouples and particle image velocimetry (PIV), respectively. They observed that velocity has a significant function in melting

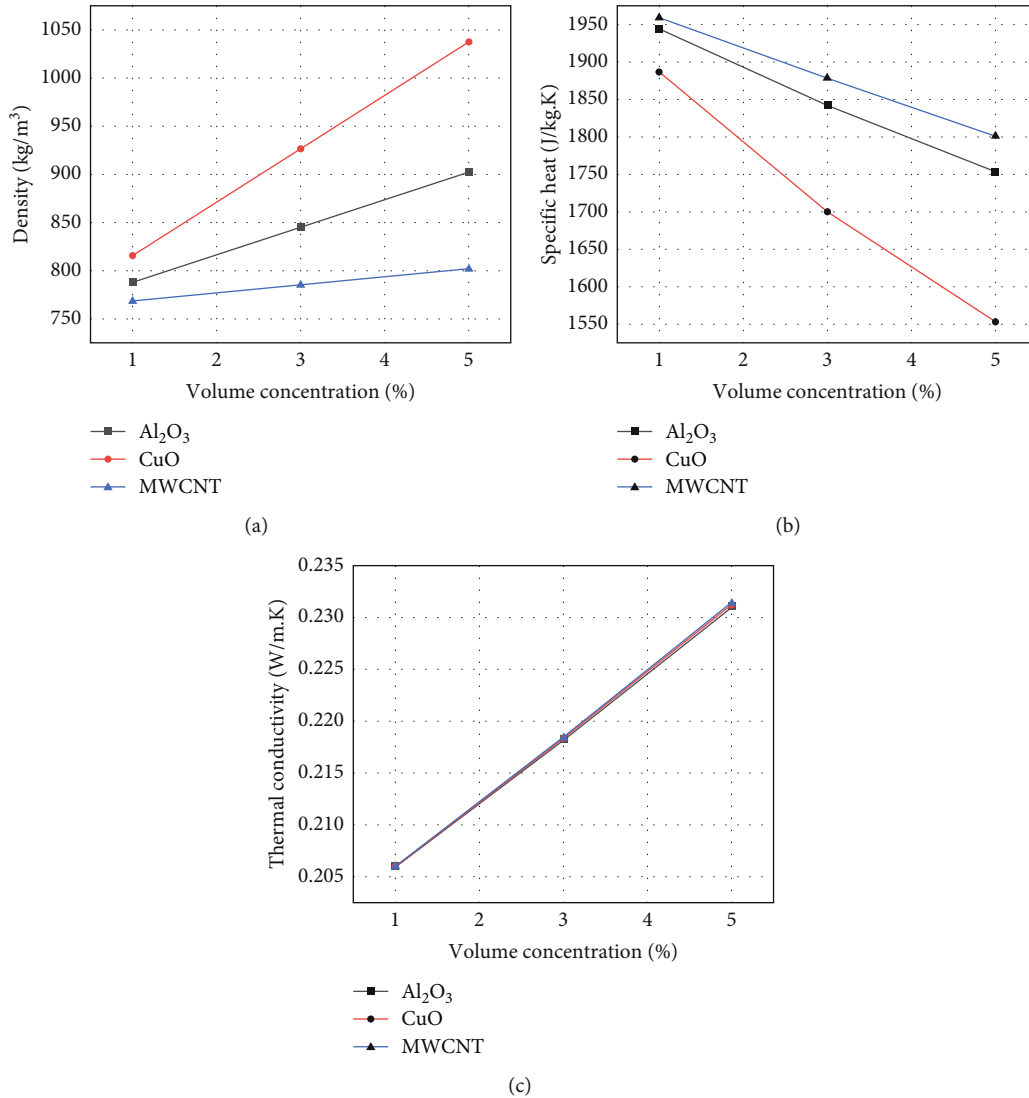


FIGURE 2: Material properties of NEPCM for different concentrations of nanoparticles. (a) Effective density. (b) Effective specific heat. (c) Effective thermal conductivity.

and heat transmission and provided the comprehensive data for heat energy transfer enhancement in numerical models with phase change process. Experimental and computational evaluations of the melting of the PCM 27 in an upright cavity were carried out by Mehdaoui et al. [25]. The simulation is carried out in TRANSYS with the Tunisian climate situations. They concluded that the room temperature with the incorporation of a PCM wall is reduced to 12°C, and the PCM has a calculated stored energy of 1200 kJ/m<sup>2</sup> by increasing 2°C in the night times. Numerical and experimental examinations are performed by Ebadi et al. [26] to understand the effect of addition of Cu nanoparticles at different Rayleigh numbers on the melting of bio-PCM in a thermal energy storage of upright cylindrical type system. They observed that adding nanoparticles has minimal effect on the shapes of melt fraction and stored energy compared to base-PCM. Further, the stored energy difference with Rayleigh numbers was very less at the start of melting, and larger

variance was detected at higher Rayleigh numbers. The effect of blending different types of nanoparticles (Silver, CuO, Al<sub>2</sub>O<sub>3</sub>, and MWCNT) with various volume fractions (1, 3, 6, 8, and 10%) into pure PCM was examined by Bashar and Siddiqui [27]. They affirmed that silver particles provide the highest heat transfer enhancement followed by CuO. The Al<sub>2</sub>O<sub>3</sub> and MWCNT nanoparticles however reduce the heat transfer due to higher settlement rates, and the optimum addition of nanoparticles suggested is 6% for 25% higher rate of melting than pure PCM. Tao et al. [28] performed the numerical investigation on the impact of filling position and free convection on the rate of charge and discharge in latent heat storage system of shell and tube type. The analysis is carried out by packing the PCM in tube side in one case and shell side in another case with and without natural convection. They observed that the heat transfer is improved by 54.2% more when the PCM is used in tube side escorted by natural mode of convection with reduced

TABLE 1: Thermophysical properties of the base materials used.

Properties	Pure PCM (RT-42)	Alumina (Al <sub>2</sub> O <sub>3</sub> )	Copper oxide (CuO)	Multiwalled carbon nanotube (MWCNT)
Density (kg/m <sup>3</sup> )	760	3600	6310	1600
Specific heat (KJ/kg.K)	2000	765	531	8.039
Thermal conductivity (W/m.K)	0.2	36	76	3000
Viscosity (kg/m.s)	0.02351	—	—	—
Thermal expansion coefficient (1/K)	0.0005	—	—	—
Pure solvent melting heat (J/kg)	165000	—	—	—
Solidus temperature (K)	311.15	—	—	—
Liquidus temperature (K)	315.15	—	—	—

TABLE 2: Number of elements vs. Nusselt number (Nu).

Grid size	Nusselt number (Nu)
61 × 61	2.10952
100 × 100	2.10201
143 × 143	2.09754
179 × 179	2.09348
200 × 200	2.08958

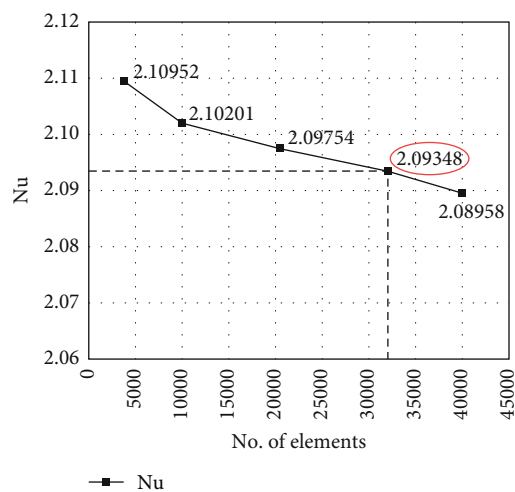


FIGURE 3: Grid independence study.

melting time of 34.4% and 36.6% more with the PCM present in tube side without the free convection at a melting rate of 25.4% compared to the PCM in shell side. Joneidi et al. [29] investigated the impact of thermal heat flux and alignment of the enclosure on the heat transmission and melt fraction of PCM filled in a rectangular container. The rectangular cavity is heated with different heat fluxes (4.4 W, 5 W, and 5.6 W) oriented in different inclinations (0°, 45°, and 90°), and the analysis was carried with the help of thermocouples and camera. They concluded that the increase in heat flux led to reduction in the rate of melting of the PCM and an increase in inclination angle results in maximization of the final stored energy. The numerical analysis of a n-

octadecane PCM filled in a container incorporated with silicone heating generating element was done by Bondareva and Sheremet [30]. The influence of Ra, St, and Ostrogradsky numbers on the speed of melting was analysed. They affirmed that the increase in all the three parameters have positive influence upon heat transmission enhancement and diminishes the time of melting. Arıcı et al. [31] investigated the impact of the volume concentration of the nanoparticles added in the PCM filled in a square cavity with varying wall temperatures. The analysis is performed with Paraffin wax, and Al<sub>2</sub>O<sub>3</sub> is employed as nanoparticles in different proportions (1%, 3%, and 5%). The results explained that the increase in volume fraction after 1% has a lower effect after 20 min of time. The orientation of the heater plays a vital role after that time than the nanoparticle concentration. Enhancement of heat transfer using PCM material inside the annular region between two concentric circular, elliptical cylindrical with different orientations inside circular cylinder, and incorporation of fin inside cylinder was studied numerically by Rabienataj Darzi et al. [32]. The analysis is also carried out with the inclusion of Cu nanoparticles in the PCM. They reported higher melting rate at the upper part of the annular segment than the lower, and the usage of upright elliptical tube orientation reduces melting time. Also, blending Cu nanoparticles improves the heat transmission, and fins positioned on the higher and lower temperature walls enhance the melting rate. Evaluation of the heat transmission process in latent thermal energy storage units filled with nano-PCM is performed by Tasnim et al. [33]. The impact of dimensionless parameters is studied using scaled analysis for complete melting of PCM. They observed that heat transmission by both conductive and convective modes was degraded by addition of nanoparticles in PCM. Experimental analysis of the enhancement of the heat transmission in a PCM-filled enclosure using different inclination angles is carried out by Kamkari et al. [34]. The PCM used in this work is lauric acid with the Ra ranging from 3.6 to 8.3 E8, and the inclination angles of 0, 45, and 90° are performed. The photographs taken are image processed in order to differentiate the solid and liquid regions, and temperatures are recorded with the

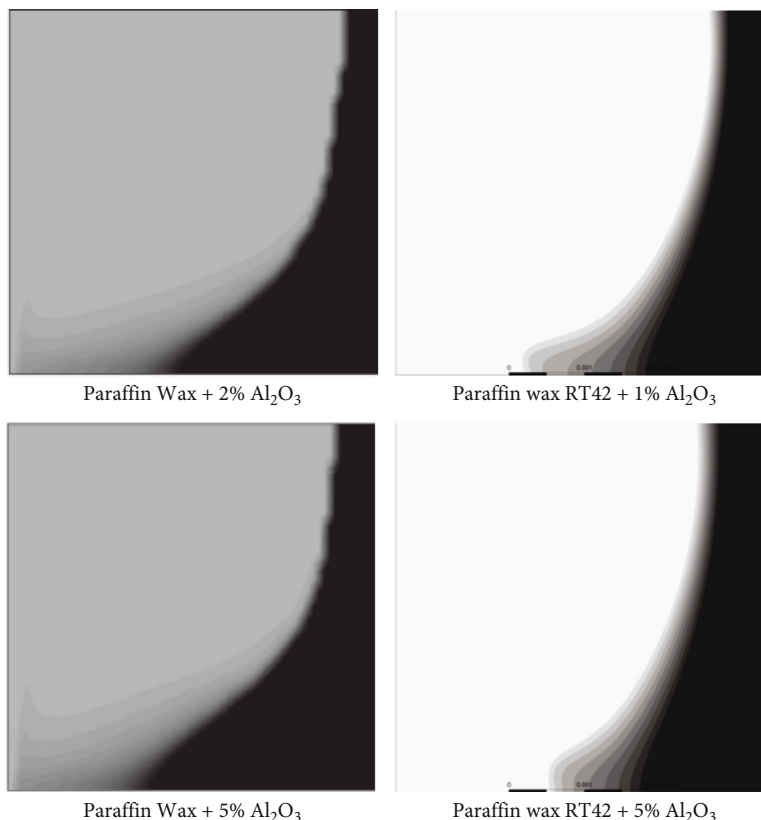


FIGURE 4: Comparison of the present work with reference work.

help of thermocouples. They noted that changing the orientation from vertical  $90^\circ$  to  $0^\circ$  will create the Benard which will affect the natural convection. Also, the rate of melting enhanced 35% and 53% for  $45^\circ$  and  $0^\circ$  compared to perpendicular orientation. The analysis of the melting rate of n-octadecane PCM using suspended CuO nanoparticles in a cavity with uniform thermal heat flux supplied to one of the edges was performed by Dhaidan et al. [35]. The influence of Ra, nanoparticle volume concentrations, and the subcooling was investigated. The PCM melting is dominated with the conduction represented as straight line shapes in the beginning, later as time marches it is shifted to natural convection curved shapes, they noted. Also, the heat transmission enhancement and rate of melting are improved upon optimum addition of nanoparticles and with increase in Ra. Bashirpour-Bonab et al. [36] numerically investigated the melting fraction of CuO-blended nano-PCM filled in a multitube heat exchanger. The impact of nanoparticle volume fraction, number of tubes, and spacing between the tubes on rate of melting is studied. They reported that the melting fraction is improved to 33.87% with 7% volume concentration and 4 number of tubes and 20.54% by increasing the distance between the tubes. The analysis of heat transfer characteristics of PCM filled in a combined fractal fin-based heat exchanger is carried out by Luo et al. [37]. The influence of combined fractal fins, fin's area, spacing, and partition between the fins is studied. The time to liquify the PCM is reduced with the fractal fins by 68%. They concluded

that the decrement of width takes a long time to raise the fin's temperature and increase the heat transfer area results in reduction of thermal resistance. However, the mean liquid fraction of PCM does not continuously rise with the area of heat transfer. Zhang et al. performed the numerical study on the thermal management of the buildings using encapsulated PCM. They focused on the effect of geometry of the encapsulation on the melting behaviour of the PCM and validated the numerical outcomes with the experimental results. Also, the variation of shell orientation, size, and temperature difference is studied. They affirmed that the pyramidal-shaped shell attains the minimum time of melting and recommended the medium size capsule with low initial temperature differences. Experimental heat transfer analysis of composite PCM prepared with lauric and palmitic acid distributed in mesoporous graphite (MG) is conducted by Nirwan et al. [38]. The impact of variation of weight fraction is studied using differential scanning calorimeters. The weight fraction of 1:5 MG-PCM composite takes away the maximum heat by reducing the temperature of the heating source by  $20^\circ\text{C}$ . They recommended this ratio of the composite rather than the pure form of PCM for maximum heat transfer in electronic devices. Li et al. [39] worked on the microencapsulation of aluminium and zinc for high-temperature thermal energy storage applications. The preparation and characterization of microencapsulated PCMs are explained. They observed that the latent heat of MEPCMs after boehmite, thermal oxidation, and copper

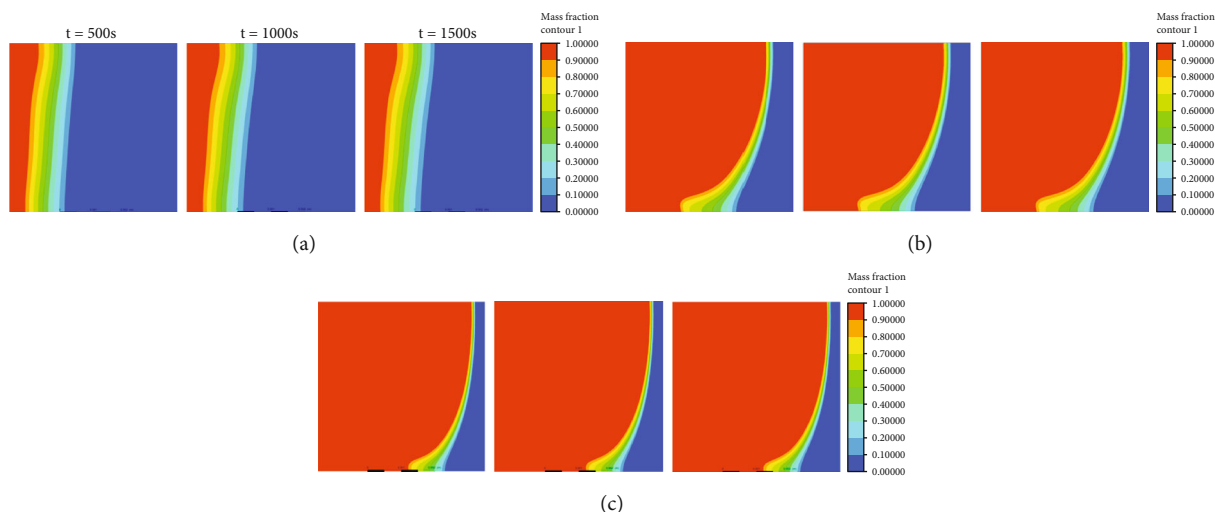


FIGURE 5: Melt-fraction contours of PCM melting for (a)  $Gr = 5000$ , (b)  $Gr = 13000$ , and (c)  $Gr = 20000$ .

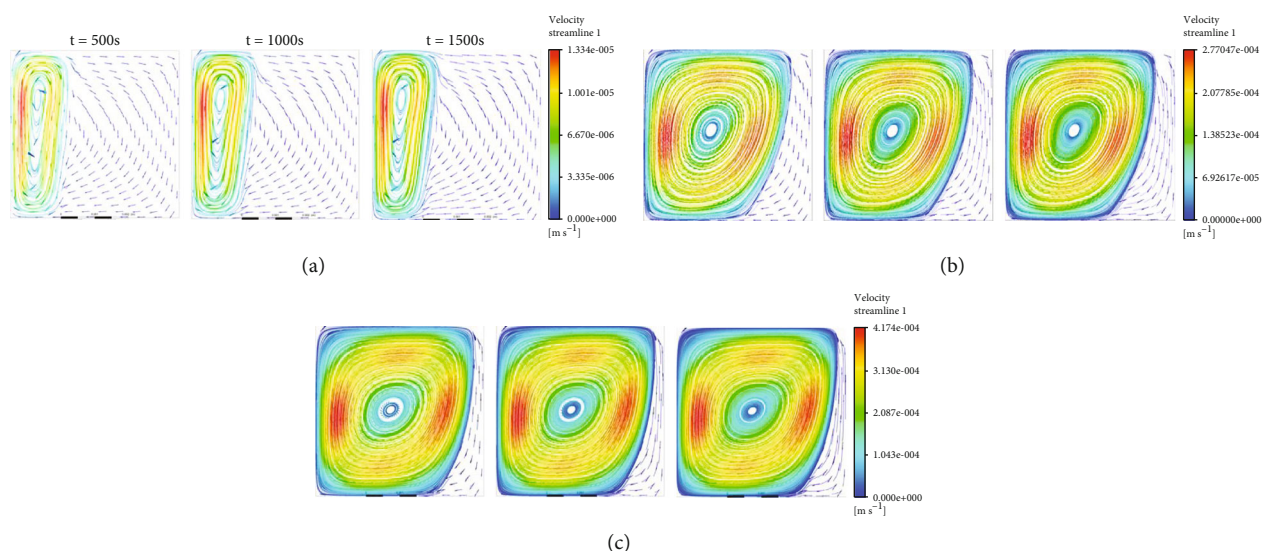


FIGURE 6: Velocity streamlines of pure PCM for  $Gr$  (a) 5000, (b) 13000, and (c) 20000.

plating treatment reduced to 160.7 J/g, 126.4 J/g, and 89 J/g from 176 J/g of pure Al-Zn MEPCM. However, they noted the life of the MEPCM has improved after the copper plating treatment. The experimental investigation of microencapsulation of  $C_{10}H_{20}O_2$  (CA) and  $C_6H_{32}O_2$  (PA) eutectic mixture in polyvinyl chloride (PVC) is carried out by Xing et al. [40]. From the characterization of the encapsulated PCM, they found that the optimum ratio of shell and core is 1:2 with the liquefaction temperature of  $17.1^\circ\text{C}$  and pure solvent melting heat of 92.1 J/g. A 500:300 nm thickness microencapsulation of  $ZnO:Al_2O_3$  composite material for medium temperature applications is prepared by Kawaguchi et al. [41]. It exhibits a melting temperature of  $510^\circ\text{C}$  with a pure solvent melting heat of 117 J/g and noted that 75% of encapsulations maintained the same spherical form after 100 cycles. Also, they sintered the MEPCM with glass frit and observed almost 100% of shape retainment after 100 cycles. Jevnikar and Siddiqui [42] performed the experimental and

numerical flow and thermal analysis of PCM. The influence of heating location on the flow field and heat transfer of PCM is studied. They noted that the melting and thermal performance of PCM is influenced by the fluid flow regulated by natural convection. Numerical analysis of the effect of vertical aluminium fins on the heat transfer enhancement of PCM is carried out by Abdi et al. [43]. They affirmed that with the usage of five numbers of long fins, a 200% of power improvement, 6% of energy storage reduction, and 12% of depletion in PCM content are observed. Kamkari and Amlashi [44] numerically investigated the impact of orientation of the enclosure on the melting performance of PCM. A reduction of 52% and 37% of melting time is observed for  $0^\circ$  and  $45^\circ$  orientations. They also presented the correlations to predict the melting rate, energy stored, and  $Nu$  at any instant. The design of PCM container with double pipe helical coiled tube for thermal energy storage application is examined numerically by Mahdi et al. [45]. They concluded that the

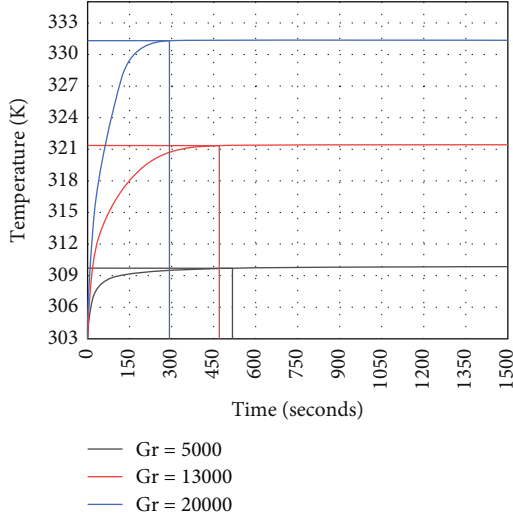


FIGURE 7: The effect of Gr on temperature of PCM with time.

proposed design reduces the melting rate by 25% and 59% compared to parallel and perpendicular double pipe energy storage systems. Also, the pitch of the coil effects incredible phase change transformation; however, they selected the optimum pitch of outer diameter as 2. The design and optimization of a multilayer shell and tube unit incorporated with longitudinal and radial metal fins are carried out by Xu et al. [46]. The amount of melting time reduced is 56%, 65%, and 71% with the addition of fins than no fin condition. The maximum reduction in time is observed for radial type of fin, and this is selected as the best arrangement. The optimum configuration increases the comprehensive storage density evaluation to 36%.

The detailed review of many researches apprises the various techniques involved in PCM-based thermal storage systems. However, only few discussed the combined effect of nanoparticle incorporation and angular orientation of the container. The main objective of this work is to study the effect of Grashof number (5000, 13000, and 20000), nanomaterial type ( $\text{Al}_2\text{O}_3$ , CuO, and MWCNT), volume concentration (0%, 1%, 3%, and 5%), and orientation angle (30, 45, and 60°) on the melting rate of the PCM in a square container. The analysis is carried out with RT42 PCM up to 1500 sec.

**1.1. Problem Description and Methodology.** A two-dimensional transient numerical analysis of the PCM filled in a square enclosure inclined in different orientations is performed. Figures 1(a) and 1(b) show the geometry description of the enclosure studied.

In this work, a square enclosure with 5 mm × 5 mm is modelled in ANSYS design modeler. This cavity is embedded by phase change material (RT-42) and consolidated with different nanoparticles ( $\text{Al}_2\text{O}_3$ , CuO, and MWCNT) by varying concentration (1%, 3%, and 5%). The top and lower walls are kept adiabatic, the left side wall is subjected to higher temperature ( $T_h$ ), and the right side wall is subjected to room temperature ( $T_c$ ) so that  $T_h > T_c$ . Transient numer-

ical study is carried out for the time steps of 500, 1000, and 1500 seconds. Also, the same analysis is executed by changing the orientation of the base side of the cavity with different inclinations (30, 45, and 60°) as shown in Figure 1(b). The governing equations for numerical computation are listed below from equations (1) to (3):

Continuity equation:

$$\frac{\partial \rho}{\partial t} + \nabla \cdot (\rho \vec{U}) = 0. \quad (1)$$

Momentum equation:

$$\frac{\partial}{\partial t} (\rho \vec{U}) + \nabla \cdot (\rho \vec{U} \vec{U}) = -\nabla P + \rho \vec{g} + \nabla \cdot \vec{\tau} + \vec{F}, \quad (2)$$

where  $\rho \vec{g}$  and  $\vec{F}$  are gravitational and external body forces, respectively.  $P$  is static pressure, and  $\vec{\tau}$  is a stress tensor.

Energy equation:

$$\frac{\partial (\rho H)}{\partial t} + \nabla \cdot (\rho \vec{U} H) = \nabla \cdot (K \nabla T) + S. \quad (3)$$

Here,  $H$ ,  $T$ ,  $\rho$ , and  $K$  are enthalpy, temperature, density, and conductivity of nanoparticle enhanced-phase change material (NEPCM), respectively.  $\vec{U}$  is velocity and  $S$ , and volumetric heat generation term is assumed zero in present analysis. The gross enthalpy of PCM  $H$  is aggregate of sensible heat ( $h$ ) and latent heat ( $\Delta H$ ), respectively. Latent heat is expressed as

$$\Delta H = \beta L, \quad (4)$$

where  $L$  is the latent heat of PCM, and  $\beta$  is the liquid fraction given by the following equation,

$$\left. \begin{aligned} \beta &= 0 & \text{if } T < T_{solidus} \\ \beta &= 1 & \text{if } T > T_{solidus} \text{ and,} \\ \beta &= \frac{T - T_{solidus}}{T_{liquidus} - T_{solidus}} & \text{if } T_{solidus} < T < T_{liquidus} \end{aligned} \right\} \quad (5)$$

Now thermophysical properties of nano-PCM such as density, heat capacity, latent heat, and viscosity are calculated using the Arasu and Mujumdar [47], Ebrahimi and Dadvand [48], and Teja et al. [49] presented from equations (6) to (9), and the variation of these properties with volume concentration is shown in Figure 2.

$$\rho_{np\text{pcm}} = \varphi \rho_{np} + (1 - \varphi) \rho_{\text{pcm}}, \quad (6)$$

$$c_{p,np\text{pcm}} = \frac{\varphi (\rho c_p)_{np} + (1 - \varphi) (\rho c_p)_{\text{pcm}}}{\rho_{np\text{pcm}}}, \quad (7)$$



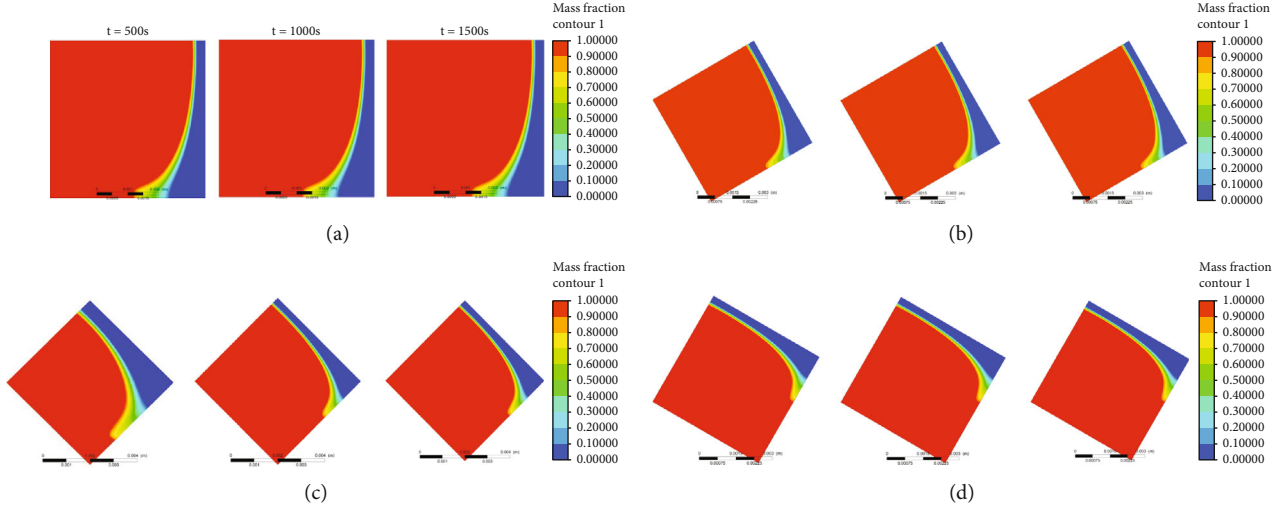


FIGURE 8: Melt-fraction contours of pure PCM in a container oriented in (a)  $0^\circ$ , (b)  $30^\circ$ , (c)  $45^\circ$ , and (d)  $60^\circ$ .

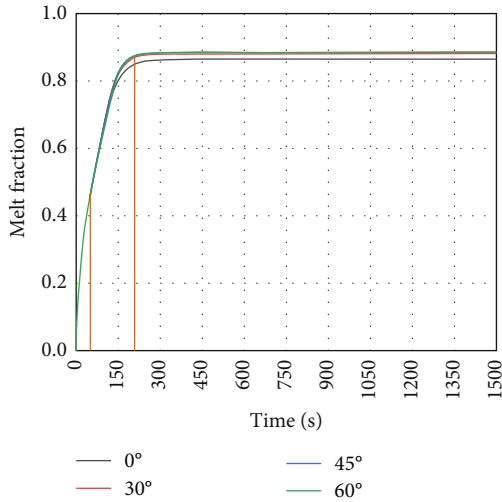


FIGURE 9: Effect of orientation on melt-fraction with time.

$$L_{npcm} = \frac{(1 - \varphi)(\rho L)_{pcm}}{\rho_{npcm}}, \quad (8)$$

$$\mu_{npcm} = 0.983e^{(12.959\varphi)} \mu_{pcm}. \quad (9)$$

While the effective thermal conductivity is expressed as

$$K_{npcm} = \frac{K_{np} + 2K_{pcm} - 2(K_{pcm} - K_{np})\varphi}{K_{np} + 2K_{pcm} + (K_{pcm} - K_{np})\varphi} K_{pcm} + 5 \times 10^4 \beta_k \zeta \varphi \rho_{pcm} C_{p,pcm} \sqrt{\frac{BT}{\rho_{np} d_{np}}} f(T, \varphi), \quad (10)$$

where  $B$  is Boltzmann constant, and its value is  $1.381 \times 10^{-23}$  J/K and,

$$\beta_k = 8.4407(100\varphi)^{-1.07304}, \quad (11)$$

$$f(T, \varphi) = (2.8217 \times 10^{-2} \varphi + 3.917 \times 10^{-3}) \frac{T}{T_{ref}} + (-3.0669 \times 10^{-2} \varphi - 3.91123 \times 10^{-3}). \quad (12)$$

Here,  $T_{ref}$  is assumed to be 303 K. The properties of NEPCM for different volume fractions (1%, 3%, and 5%) of nanoparticles ( $Al_2O_3$ , CuO, and MWCNT) are calculated using the equations (6) to (10). The thermophysical properties of the base materials are listed in Table 1. Also, the dimensionless Grashoff number and Nusselt number used are expressed as

$$Gr = \frac{g\beta_f(T_h - T_c)H^3}{\nu_f^2}, \quad (13)$$

$$Nu = \frac{hL}{K}. \quad (14)$$

The boundary conditions applied to the model in the study is mathematically given by:

$$T = T_h \text{ for } X = 0 \text{ and } 0 < Y < 5 \text{ on left vertical wall.}$$

$$T = T_c \text{ for } X = 5 \text{ and } 0 < Y < 5 \text{ on right vertical wall.}$$

$dQ = 0$  for  $0 < X < 5$  and  $Y = 0$  on bottom horizontal wall.

$$dQ = 0 \text{ for } 0 < X < 5 \text{ and } Y = 5 \text{ on top horizontal wall.}$$

**1.2. Numerical Procedure.** In the present study, numerical analysis is carried out with ANSYS FLUENT software. The governing equations based on boundary conditions are numerically solved by fluent using FVM. Construction of geometry is done in a design modeler from the fluid flow (fluent) geometry component. Meshing of the model is done by taking an adaptive size function with a fine relevance center. The skewness for mesh is maintained minimum while the orthogonal quality is kept closer to 1 by incorporating quadrilateral mesh cells by setting quadrilaterals as the meshing method.

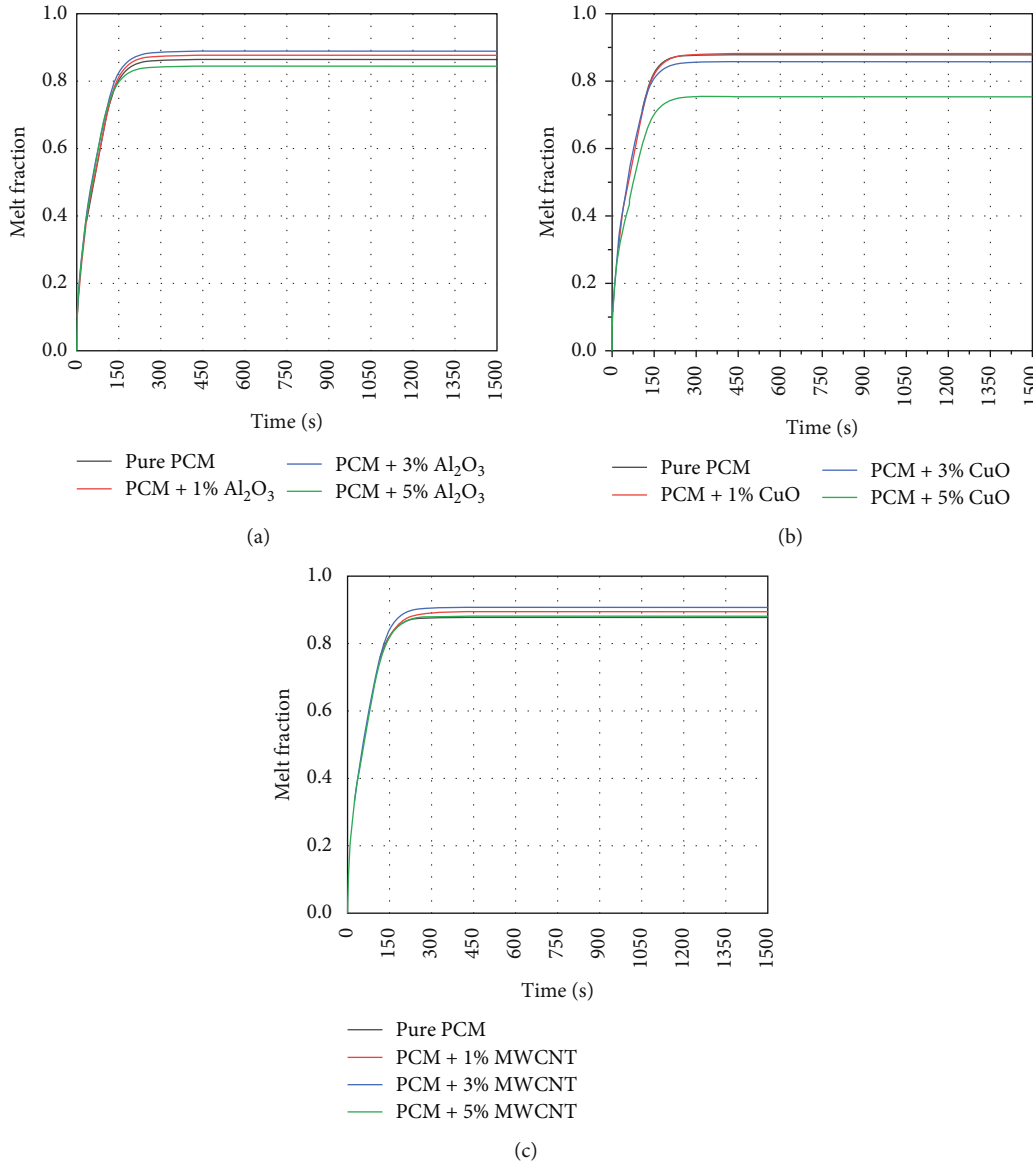


FIGURE 10: Effect of nanoparticles (a)  $Al_2O_3$ , (b)  $CuO$ , and (c)  $MWCNT$  with different volume concentrations (1%, 3%, and 5%) on melt fraction at  $Gr = 20000$ .

Pressure-based solver along with its velocity coupling and adjustment equation is utilized with simple algorithms and PRESTO! Scheme, respectively. While the equations of momentum and energy are evaluated using an upwind scheme of second order. Transient analysis is performed by taking the time step size as 0.2 s, and the maximum number of iterations is fixed as 20 for every time step. The convergence limit for residuals is fixed as  $10^{-3}$  for continuity, momentum equations, and it is  $10^{-6}$  for an energy equation.

**1.3. Grid Independence Study and Validation.** To select the appropriate grid size, the numerical model is verified with different element sizes. The mesh consists of uniform quadrilaterals distribution throughout the enclosure. Five different mesh sizes were examined with the number of cells varying from  $61 \times 61$ ,  $100 \times 100$ ,  $143 \times 143$ ,  $179 \times 179$ , and  $200 \times 200$ , respectively, as shown in Table 2. As shown in

Figure 3, the difference in the Nusselt numbers for  $179 \times 179$  (32041 elements) and  $200 \times 200$  (40000 elements) is very small. Hence, the number of cells in the mesh is selected as 32041 with element size as 0.028 mm for further study.

The validation of the present work is conducted qualitatively by comparing the melt-fraction contours of the present study with Arasu and Mujumdar [47] study. Comparison is done for melting of PCM (Paraffin wax) with 2%, 5%  $Al_2O_3$  addition and melting of PCM (RT-42) with 1%, 5%  $Al_2O_3$  addition of present study. The contours of the melt fraction for both the current work and reference work are matching very nearer as shown in Figure 4.

**2. Results and Discussion**

Computational thermal analysis of heat transfer and melting of pure PCM/nano-PCM (PCM + nanoparticles) is carried

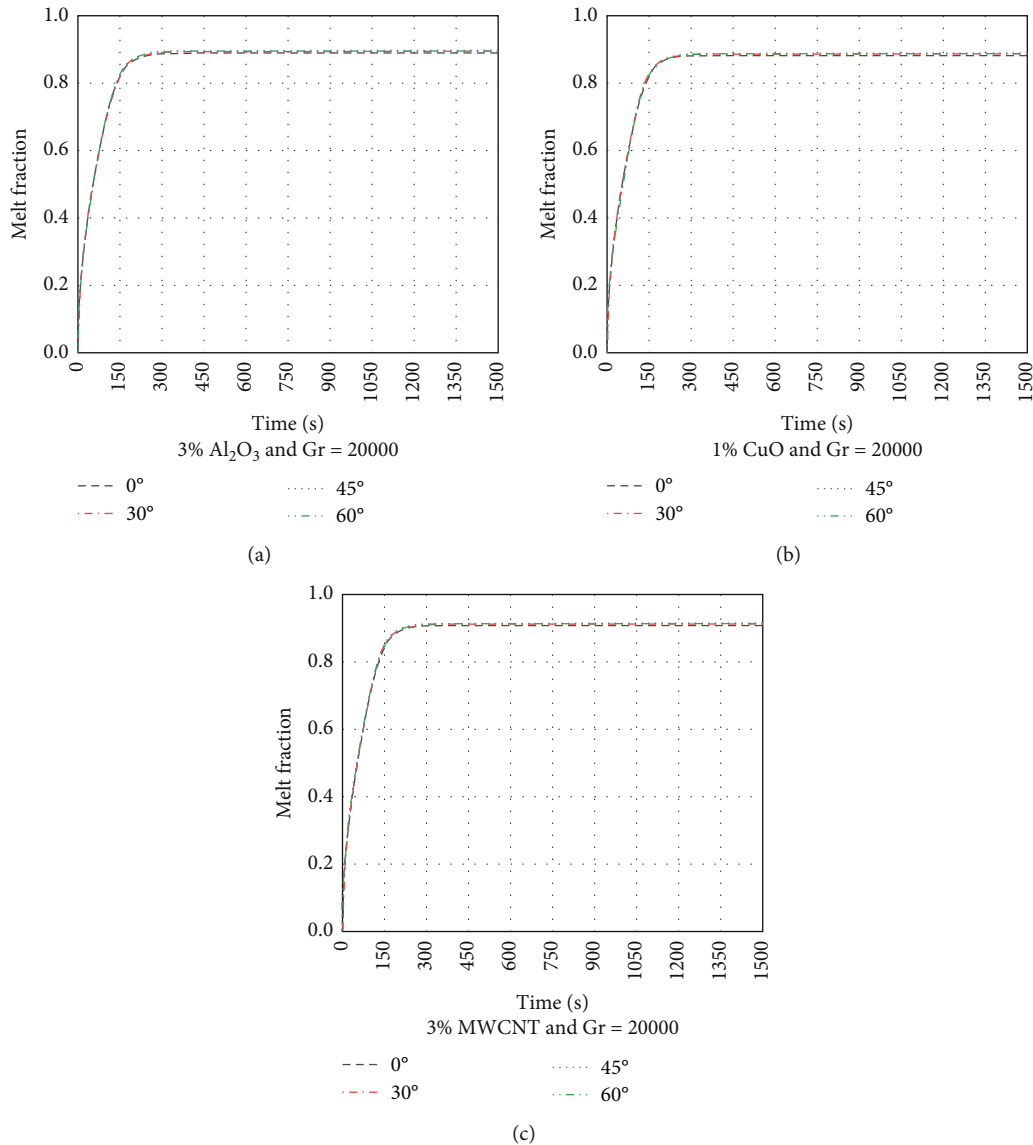


FIGURE 11: Effect of orientation in (a) PCM + 3%  $\text{Al}_2\text{O}_3$ , (b) PCM + 1% CuO, and (c) PCM + 3% MWCNT based nanofluids on melt fraction at Gr = 20000.

out for three different Grashoff numbers (5000, 13000, and 20000) given to left side wall with the bottom edge oriented in different inclinations ( $0^\circ$ ,  $30^\circ$ ,  $45^\circ$ , and  $60^\circ$ ). The effect of nanoparticle type ( $\text{Al}_2\text{O}_3$ , CuO, and MWCNT), concentration (1%, 3%, and 5%), Grashoff number, and inclination is presented.

**2.1. Melting of Pure PCM.** Figures 5(a)–5(c) show the melt fraction contours of the PCM at three different Grashoff numbers up to 1500 sec with an interval of 500 sec. Red portion in the contour represents the liquefied part of the PCM with a melt fraction as 1.0, and the solid part is described as the blue portion with a melt fraction as 0.0. In between, the different colours of the contours represent the mushy region. It is observed that during the initial stages of melting, the liquid-fraction region is almost vertical as shown in

Figure 5(a). This clearly shows that the initial mode of heat transfer was by conduction. After some time, the conduction dominant zone is converted into mixed conduction and convection zone by transforming the solid PCM into liquid. The density difference between the solid and liquid makes the material move by natural convection as shown in Figures 6(a)–6(c) for different Gr.

The movement of the liquid will form upward and downward rotations with small velocities due to the buoyancy forces formed by the temperature difference between hot and cold wall. Also, due to the boundary layer effect by viscosity, the velocity adjacent to the wall is zero, and it gradually increases away from the wall up to the solid portion of the PCM.

With the increase in Gr, the rise in hot wall temperature is evident, and the availability of melted PCM will be more;

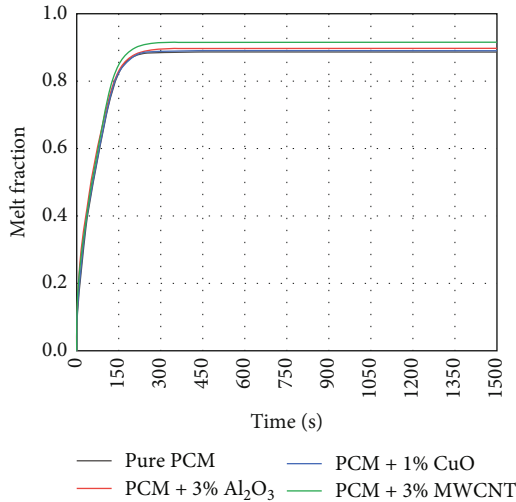


FIGURE 12: Comparison of melt fraction for 45° oriented enclosure for different nano-PCM at  $Gr = 20000$ .

therefore, more velocity has been observed. For  $Gr = 20000$ , the highest velocity noted is  $4.174e-4$  m/s which is 51.23% and 32.97% higher than  $Gr = 5000$  and 13000 case.

Figure 7 depicts the effect of  $Gr$  on the temperature of the PCM with respect to time. It is noted that the temperature has been increased with  $Gr$  for a period of time; afterward, it comes to a steady state. It is also identified that the slope of the temperature lines are reducing with respect to  $Gr$ , indicating that the rate of attaining steady state is less with increase in  $Gr$ . The amount of heat transferred to the PCM is stored in the form of phase change. With the increase in temperature, the amount of melting rate also improved from 24.16% to 25.44%, 76% to 76.35%, and 86.4% to 86.417% for  $Gr = 5000$ , 13000, and 20000, respectively. For the same time period, the melted region is more for  $Gr = 20000$ .

**2.2. Melting of PCM in an Enclosure with Angular Orientations.** Transient thermal analysis of a square enclosure filled with the PCM, oriented in different angles ( $0^\circ$ ,  $30^\circ$ ,  $45^\circ$ , and  $60^\circ$ ), as shown in Figure 1 is performed. Figure 8 shows the melt-fraction contours for different  $Gr$  (5000, 13000, and 20000) and varying time intervals (500 s, 1000 s, and 1500 s).

Figure 9 represents the graph plotted for the variation of melt-fraction of PCM with different orientations ( $0^\circ$ ,  $30^\circ$ ,  $45^\circ$ , and  $60^\circ$ ) for a time of 1500 seconds and  $Gr$  of 20,000. In the beginning, at around 50 seconds, the PCM in all the containers is in the same stage, the PCM is slowly melting into fluid up to 200 seconds, and later, the material in all the containers attains the steady state. It is observed that the amount of melt is more as the inclination angle increases. The percentage increase of melt fraction is less for different orientations and pure PCM. Using  $60^\circ$  orientation, the melt fraction improved is 2.43%, 0.5%, and 0.08% more than the  $0^\circ$ ,  $30^\circ$ , and  $45^\circ$  inclinations.

**2.3. Effect of Nanoparticle Concentration in PCM.** The computational analysis on the melting performance of phase change material blended with different nanoparticles ( $Al_2O_3$ /CuO/MWCNT) in various proportions (1%, 3%, and 5%) filled in a square enclosure is carried out. Figures 10(a)–10(c) show the comparison of the melt fraction of nano PCM (PCM +  $Al_2O_3$ /CuO/MWCNT) with different concentrations (1%, 3%, and 5%), respectively. It is clearly visible that the amount of melt fraction is not varied linearly with the volume concentration of the nanomaterial. In the first case with  $Al_2O_3$ , the maximum melt fraction is observed for PCM + 3% followed by 1%, pure PCM (0%), and 5%. The melting performance is improved with addition of  $Al_2O_3$  up to 3%; afterward, it is reduced. This is because of increased density and viscosity. Also, in the beginning of heating PCM, the transfer of energy is predominantly by conduction succeeded by convection. By adding more amounts of high conductive nanomaterials, the heat transfer will again convert into a conductive zone. Therefore, the melting performance reduces.

With 3%  $Al_2O_3$ , the increase in fluid fraction is 2.9%, 1.38%, and 5.27% more than the melt fraction of 1%, pure PCM, and 5% added nanofluid, respectively. In the second case, in Figure 10(b), though the conductivity of the CuO is more than  $Al_2O_3$ , the enhancement of effective thermal conductivity is very less compared to effective density. Hence, 1% CuO nanomaterial addition has more amount of liquid fraction than 3 and 5% nanofluid. Figure 2 shows the variation of thermophysical properties of nanofluids for different nanoparticle concentration. With 1% CuO, increase in fluid fraction is 2%, 2.924%, and 11% higher than the melt fraction of 3%, pure PCM, and 5% added nano-PCM. With the incorporation of MWCNT nanoparticles (1%, 3%, and 5%) shown in Figure 10(c), the heat transfer is enhanced due to high effective conductivity of the nanofluid, and also the percentage of change in density is less compared to other two nanoparticles. Similar to  $Al_2O_3$ -based nano-PCM, the liquid fraction is more in 3% followed by 1% addition. However, the melt fraction is less in 5% MWCNT due to the effect of thermophysical properties. The increase in fluid fraction of nanofluid blended with 3% MWCNT is 5%, 1.46%, and 2.94% more than pure PCM, 1%, and 5% blended nano-PCM.

**2.4. Effect of Orientation and Nanoparticles on Melt Fraction of Nano-PCM.** Combining the effect of angular orientation of the enclosure and nanomaterial added to the fluid on the melt-fraction of NEPCM is studied. Figures 11(a)–11(c) represent the graph plotted between time and melt fraction for different inclinations ( $0^\circ$ ,  $30^\circ$ ,  $45^\circ$ , and  $60^\circ$ ) of enclosure filled with 3%  $Al_2O_3$ , 1% CuO, and 3% MWCNT blended nano-PCM, respectively.

The volume concentration compared is chosen on the basis of the maximum melt fraction with each nanomaterial. It is observed that the utmost amount of melt is occurring in a container with an orientation of  $45^\circ$  for all the nanofluids, despite having marginal change in liquid fraction. Therefore, it is concluded that the effect of enclosure orientation is

negligible compared with the effect of volume fraction of the nanoparticles.

From Figure 12, it is noted that among  $\text{Al}_2\text{O}_3$ , CuO, and MWCNT with different concentrations (pure PCM (0%), 1%, 3%, and 5%) blended with the PCM of RT 42 and orientations ( $0^\circ$ ,  $30^\circ$ ,  $45^\circ$ , and  $60^\circ$ ), the maximum amount of heat transfer and liquid fraction is attained for (PCM + 3% MWCNT) nano-PCM oriented with  $45^\circ$ . With the incorporation of 3% MWCNT/PCM in  $45^\circ$  orientated enclosure, an improvement of 3.4%, 2.04%, and 2.94% melt performance than pure PCM, (PCM/3%  $\text{Al}_2\text{O}_3$ ), (PCM/1% CuO), respectively, is noted.

This is because the changes in the thermophysical properties of the MWCNT blended PCM are more substantial than the other nanoparticle concentrated PCM. Also, due to symmetry and less buoyancy effects compared to other orientations, the liquid fraction in  $45^\circ$  orientation is more.

### 3. Conclusions

Numerical analysis on the effect of nanoparticle type ( $\text{Al}_2\text{O}_3$ , CuO, MWCNT), volume concentration (0%, 1%, 3%, and 5%), and angular orientation of the enclosure ( $0^\circ$ ,  $30^\circ$ ,  $45^\circ$ , and  $60^\circ$ ) on the melting of phase change material RT 42 is carried out.

It is observed that

- (i) For the melting of the pure PCM, it is affirmed that the temperature of the heat source is increased with increase in Gr (5000, 13000, and 20000). Due to this, the heat transfer and melting rate have been enhanced
- (ii) The maximum melting fraction is identified for Gr = 20000. Also, the shape of the melted portion is changed from vertical to parabolic curvature profile indicating that the mode of heat transfer is changed to convection from conduction
- (iii) The material properties of phase change material consolidated with nanoparticles ( $\text{Al}_2\text{O}_3$ , CuO, and MWCNT) into RT 42 PCM are presented. With increase in volume concentration (1%, 3%, and 5%) of the nanoparticles, the effective density, thermal conductivity, and viscosity are increased, while specific heat and latent heat are reduced. The rise in thermal conductivity is very less compared to all other properties
- (iv) The liquid fraction content is not varied linearly with respect to volume concentration of the nanoparticles. Comparing pure PCM, greater rate of melting is achieved in 3%  $\text{Al}_2\text{O}_3$  and MWCNT, 1% CuO. With 3%  $\text{Al}_2\text{O}_3$ , the increase in fluid fraction is 2.9%, 1.38%, and 5.27% more than the melt fraction of 1%, pure PCM, and 5% added nanofluid, respectively. With 1% CuO, increase in fluid fraction is 2%, 2.924%, and 11% higher than the melt fraction of 3%, pure phase change material, and 5% added NEPCM. The enhancement in the

fluid fraction of nanofluid blended with 3% MWCNT is 5%, 1.46%, and 2.94% more than pure PCM, 1%, and 5% blended nano-PCM

- (v) Increasing volume fraction beyond the optimum level reduces the melting performance. This is because of the relative escalation of viscous forces than the buoyancy forces with increase in volume fraction. Also, the convection dominant heat transfer will be shifted to conduction state again
- (vi) The enclosure orientation has very negligible effects on the advancement of the melt for both phase change material and NEPCM fluids. In case of pure phase change material, the maximum liquid fraction is seen for a  $60^\circ$  oriented container, while it is a  $45^\circ$  orientation for a nano-PCM case
- (vii) Among all the nanoparticles, MWCNT-based nanofluids have a high melting rate. This is mainly because of the substantial development of thermophysical properties of MWCNT than all other nanoparticles blended PCM
- (viii) Considering all the effects, the 3% MWCNT nano-PCM oriented in  $45^\circ$  is achieving a larger fraction of melting portion. With the 3% MWCNT/PCM filled enclosure oriented in  $45^\circ$ , an improvement of 3.4%, 2.04%, and 2.94% melt performance than pure PCM, (PCM/3%  $\text{Al}_2\text{O}_3$ ), (PCM/1% CuO), respectively, is noted

### Nomenclature

NEPCM:	Nanoparticle-enhanced PCM
TES:	Thermal energy storage system
HTF:	Heat transfer fluid
RT42:	Rubitherm 42
$\rho$ :	Density
$\phi$ :	Volume concentration
$C_p$ :	Specific heat capacity
$L$ :	Latent heat
$\mu$ :	Coefficient of viscosity
$K$ :	Thermal conductivity
$\beta$ :	Volume expansion coefficient
$\text{Al}_2\text{O}_3$ :	Aluminium oxide
CuO:	Copper oxide
MWCNT:	Multiwalled carbon nanotube
$T_{\text{solidus}}$ :	Solidus temperature
$T_{\text{liquidus}}$ :	Liquidus temperature
$T_{\text{ref}}$ :	Reference temperature
Gr:	Grashof number.

### Data Availability

No data were used to support this study.

### Conflicts of Interest

The authors declare that they have no conflicts of interest.

## References

- [1] A. K. Gupta, G. Mishra, and S. Singh, "Numerical study of MWCNT enhanced PCM melting through a heated undulated wall in the latent heat storage unit," *Thermal Science and Engineering Progress*, vol. 27, article 101172, 2022.
- [2] C. Xu, M. Liu, S. Jiao, H. Tang, and J. Yan, "Experimental study and analytical modeling on the thermocline hot water storage tank with radial plate-type diffuser," *International Journal of Heat and Mass Transfer*, vol. 186, 2022.
- [3] K. Jiao, L. Lu, T. Wen, and Q. Wang, "A modified mixture theory for one-dimensional melting of pure PCM and PCM/metal foam composite: numerical analysis and experiment validation," *International Journal of Heat and Mass Transfer*, vol. 186, p. 122461, 2022.
- [4] J. S. Baruah, V. Athawale, P. Rath, and A. Bhattacharya, "Melting and energy storage characteristics of macro-encapsulated PCM-metal foam system," *International Journal of Heat and Mass Transfer*, vol. 182, p. 121993, 2022.
- [5] Y. Zhang, M. Vahabzadeh, J. F. Torres, Y. Zhao, and X. Wang, "Dynamic melting of encapsulated PCM in various geometries driven by natural convection of surrounding air: a modelling-based parametric study," *Journal of Energy Storage*, vol. 48, article 103975, 2022.
- [6] P. Huang, G. Wei, L. Cui, C. Xu, and X. Du, "Numerical investigation of a dual-PCM heat sink using low melting point alloy and paraffin," *Applied Thermal Engineering*, vol. 189, article 116702, 2021.
- [7] J. Guo, Z. Liu, Z. Du, J. Yu, X. Yang, and J. Yan, "Effect of fin-metal foam structure on thermal energy storage: an experimental study," *Renewable Energy*, vol. 172, pp. 57–70, 2021.
- [8] C. Nie, J. Liu, and S. Deng, "Effect of geometry modification on the thermal response of composite metal foam/phase change material for thermal energy storage," *International Journal of Heat and Mass Transfer*, vol. 165, article 120652, 2021.
- [9] M. Li, Q. Cao, H. Pan, X. Wang, and Z. Lin, "Effect of melting point on thermodynamics of thin PCM reinforced residential frame walls in different climate zones," *Applied Thermal Engineering*, vol. 188, article 116615, 2021.
- [10] X. Huang, C. Sun, Z. Chen, and Y. Han, "Experimental and numerical studies on melting process of phase change materials (PCMs) embedded in open-cells metal foams," *International Journal of Thermal Sciences*, vol. 170, article 107151, 2021.
- [11] A. R. Abdulmunem, P. Mohd Samin, H. Abdul Rahman, H. A. Hussien, I. Izmi Mazali, and H. Ghazali, "Numerical and experimental analysis of the tilt angle's effects on the characteristics of the melting process of PCM-based as PV cell's backside heat sink," *Renewable Energy*, vol. 173, pp. 520–530, 2021.
- [12] M. S. Mahdi, H. B. Mahood, A. N. Campbell, and A. A. Khadom, "Natural convection improvement of PCM melting in partition latent heat energy storage: numerical study with experimental validation," *International Communications in Heat and Mass Transfer*, vol. 126, article 105463, 2021.
- [13] G. S. Sodhi and P. Muthukumar, "Compound charging and discharging enhancement in multi-PCM system using non-uniform fin distribution," *Renewable Energy*, vol. 171, pp. 299–314, 2021.
- [14] M. T. Chaichan, H. A. Kazem, A. H. A. Al-Waeli, and K. Sopian, "Controlling the melting and solidification points temperature of PCMs on the performance and economic return of the water-cooled photovoltaic thermal system," *Solar Energy*, vol. 224, pp. 1344–1357, 2021.
- [15] E. Ozbas, S. Selimli, M. Ozkaymak, and A. S. S. Frej, "Evaluation of internal structure modifications effect of two-phase closed thermosyphon on performance: an experimental study," *Solar Energy*, vol. 224, pp. 1326–1332, 2021.
- [16] H. Qin, Z. Wang, W. Heng, Z. Liu, and P. Li, "Numerical study of melting and heat transfer of PCM in a rectangular cavity with bilateral flow boundary conditions," *Case Studies in Thermal Engineering*, vol. 27, article 101183, 2021.
- [17] H. Bashirpour-Bonab, "Investigation and optimization of PCM melting with nanoparticle in a multi-tube thermal energy storage system," *Case Studies in Thermal Engineering*, vol. 28, article 101643, 2021.
- [18] L. N. Gollapudi, R. Senanayake, C. Georgantopoulou, and A. K. Singh, "Numerical heat transfer analysis of a thermal energy storage system enclosure with horizontal fin for sustainable energy storage," *Case Studies in Thermal Engineering*, vol. 28, article 101670, 2021.
- [19] R. De Césaró Oliveski, F. Becker, L. A. O. Rocha, C. Biserni, and G. E. S. Eberhardt, "Design of fin structures for phase change material (PCM) melting process in rectangular cavities," *Journal of Energy Storage*, vol. 35, article 102337, 2021.
- [20] A. Abidi, M. Rawa, Y. Khetib, H. F. A. Sindi, M. Sharifpur, and G. Cheraghian, "Simulation of melting and solidification of graphene nanoparticles-PCM inside a dual tube heat exchanger with extended surface," *Journal of Energy Storage*, vol. 44, article 103265, 2021.
- [21] K. Hosseinzadeh, M. A. Erfani Moghaddam, A. Asadi et al., "Effect of two different fins (longitudinal-tree like) and hybrid nanoparticles (MoS<sub>2</sub>-TiO<sub>2</sub>) on solidification process in triplex latent heat thermal energy storage system," *Alexandria Engineering Journal*, vol. 60, no. 1, pp. 1967–1979, 2021.
- [22] B. Kok, "Examining effects of special heat transfer fins designed for the melting process of PCM and nano-PCM," *Applied Thermal Engineering*, vol. 170, 2020.
- [23] N. Dora, A. R. Mohammad, and R. Chigurupati, "Numerical model development for the prediction of thermal energy storage system performance: CFD study," *International Journal of Energy and Environmental Engineering*, vol. 12, no. 1, pp. 87–100, 2020.
- [24] S. Jevnikar and K. Siddiqui, "Investigation of the influence of heat source orientation on the transient flow behavior during PCM melting using particle image velocimetry," *Journal of Energy Storage*, vol. 25, article 100825, 2019.
- [25] F. Mehdaoui, M. Hazami, H. Taghouti, M. Noro, R. Lazzarin, and A. A. Guizani, "An experimental and a numerical analysis of the dynamic behavior of PCM-27 included inside a vertical enclosure: application in space heating purposes," *International Journal of Thermal Sciences*, vol. 133, pp. 252–265, 2018.
- [26] S. Ebadi, S. H. Tasnim, A. A. Aliabadi, and S. Mahmud, "Melting of nano-PCM inside a cylindrical thermal energy storage system: numerical study with experimental verification," *Energy Conversion and Management*, vol. 166, pp. 241–259, 2018.
- [27] M. Bashar and K. Siddiqui, "Experimental investigation of transient melting and heat transfer behavior of nanoparticle-enriched PCM in a rectangular enclosure," *Journal of Energy Storage*, vol. 18, pp. 485–497, 2018.
- [28] Y. B. Tao, Y. K. Liu, and Y. L. He, "Effects of PCM arrangement and natural convection on charging and discharging

- performance of shell-and-tube LHS unit," *International Journal of Heat and Mass Transfer*, vol. 115, pp. 99–107, 2017.
- [29] M. H. Joneidi, M. J. Hosseini, A. A. Ranjbar, and R. Bahrampoury, "Experimental investigation of phase change in a cavity for varying heat flux and inclination angles," *Experimental Thermal and Fluid Science*, vol. 88, pp. 594–607, 2017.
- [30] N. S. Bondareva and M. A. Sheremet, "Flow and heat transfer evolution of PCM due to natural convection melting in a square cavity with a local heater," *International Journal of Mechanical Sciences*, vol. 134, pp. 610–619, 2017.
- [31] M. Arıcı, E. Tütüncü, M. Kan, and H. Karabay, "Melting of nanoparticle-enhanced paraffin wax in a rectangular enclosure with partially active walls," *International Journal of Heat and Mass Transfer*, vol. 104, pp. 7–17, 2017.
- [32] A. A. Rabienataj Darzi, M. Jourabian, and M. Farhadi, "Melting and solidification of PCM enhanced by radial conductive fins and nanoparticles in cylindrical annulus," *Energy Conversion and Management*, vol. 118, pp. 253–263, 2016.
- [33] S. H. Tasnim, R. Hossain, S. Mahmud, and A. Dutta, "Convection effect on the melting process of nano-PCM inside porous enclosure," *International Journal of Heat and Mass Transfer*, vol. 85, pp. 206–220, 2015.
- [34] B. Kamkari, H. Shokouhmand, and F. Bruno, "Experimental investigation of the effect of inclination angle on convection-driven melting of phase change material in a rectangular enclosure," *International Journal of Heat and Mass Transfer*, vol. 72, pp. 186–200, 2014.
- [35] N. S. Dhaidan, J. M. Khodadadi, T. A. Al-Hattab, and S. M. Al-Mashat, "Experimental and numerical investigation of melting of phase change material/nanoparticle suspensions in a square container subjected to a constant heat flux," *International Journal of Heat and Mass Transfer*, vol. 66, pp. 672–683, 2013.
- [36] H. Bashirpour-Bonab, "Investigation and optimization of PCM melting with nanoparticle in a multi-tube thermal energy storage system," *Case Studies in Thermal Engineering*, vol. 28, p. 101643, 2021.
- [37] X. Luo, J. Gu, H. Ma et al., "Numerical study on enhanced melting heat transfer of PCM by the combined fractal fins," *Journal of Energy Storage*, vol. 45, p. 103780, 2022.
- [38] A. Nirwan, D. Gupta, R. Matta, R. Kumar, and B. Mondal, "Evaluation of heat transfer performance of PCM based composites for thermal management of electronics," *Materials Today: Proceedings*, vol. 57, pp. 954–957, 2022.
- [39] Q. Li, X. Ma, X. Zhang, J. Ma, X. Hu, and Y. Lan, "Microencapsulation of Al-Zn alloy as phase change materials for high-temperature thermal storage application," *Materials Letters*, vol. 308, p. 131208, 2022.
- [40] J. Xing, Y. Zhou, K. Yang et al., "Microencapsulation of fatty acid eutectic with polyvinyl chloride shell used for thermal energy storage," *Journal of Energy Storage*, vol. 34, p. 101998, 2021.
- [41] T. Kawaguchi, H. Sakai, N. Sheng, A. Kurniawan, and T. Nomura, "Microencapsulation of Zn-Al alloy as a new phase change material for middle- high-temperature thermal energy storage applications," *Applied Energy*, vol. 276, p. 115487, 2020.
- [42] S. Jevnikar and K. Siddiqui, "Investigation of the influence of heat source orientation on the transient flow behavior during PCM melting using particle image velocimetry," *Journal of Energy Storage*, vol. 25, article 100825, 2019.
- [43] A. Abdi, V. Martin, and J. N. Chiu, "Numerical investigation of melting in a cavity with vertically oriented fins," *Applied Energy*, vol. 235, pp. 1027–1040, 2019.
- [44] B. Kamkari and H. J. Amlashi, "Numerical simulation and experimental verification of constrained melting of phase change material in inclined rectangular enclosures," *International Communications in Heat and Mass Transfer*, vol. 88, pp. 211–219, 2017.
- [45] M. S. Mahdi, H. B. Mahood, J. M. Mahdi, A. A. Khadom, and A. N. Campbell, "Improved PCM melting in a thermal energy storage system of double-pipe helical-coil tube," *Energy Conversion and Management*, vol. 203, article 112238, 2020.
- [46] H. Xu, N. Wang, C. Zhang, Z. Qu, and M. Cao, "Optimization on the melting performance of triplex-layer PCMs in a horizontal finned shell and tube thermal energy storage unit," *Applied Thermal Engineering*, vol. 176, article 115409, 2020.
- [47] A. V. Arasu and A. S. Mujumdar, "Numerical study on melting of paraffin wax with  $\text{Al}_2\text{O}_3$  in a square enclosure," *International Communications in Heat and Mass Transfer*, vol. 39, no. 1, pp. 8–16, 2012.
- [48] A. Ebrahimi and A. Dadvand, "Simulation of melting of a nano-enhanced phase change material (NePCM) in a square cavity with two heat source-sink pairs," *Alexandria Engineering Journal*, vol. 54, no. 4, pp. 1003–1017, 2015.
- [49] P. N. S. Teja, S. K. Gugulothu, G. R. Sastry, B. Burra, and S. S. Bhurat, "Numerical analysis of nanomaterial-based sustainable latent heat thermal energy storage system by improving thermal characteristics of phase change material," *Environmental Science and Pollution Research*, vol. 18, pp. 1–14, 2021.